

Neutron Powder Diffraction Study and Physical Characterization of Zeolite D-Rho Shallow-Bed Calcined in Steam at 773 K

BY REINHARD X. FISCHER*

Central Research and Development Department,† E. I. du Pont de Nemours and Company,
Experimental Station, Wilmington, Delaware 19898, USA

WERNER H. BAUR

Institut für Kristallographie und Mineralogie der Universität, Senckenberganlage 30,
D-6000 Frankfurt am Main 11, Federal Republic of Germany

ROBERT D. SHANNON, RALPH H. STALEY, LLOYD ABRAMS AND ALEXANDER J. VEGA

Central Research and Development Department, E. I. du Pont de Nemours and Company,
Experimental Station, Wilmington, Delaware 19898, USA

AND JAMES D. JORGENSEN

Materials Science Division, Argonne National Laboratory, Argonne, Illinois 60439, USA

(Received 20 June 1987; accepted 20 January 1988)

Abstract

Zeolite Rho samples, shallow-bed calcined in steam at 773 K, were studied by time-of-flight neutron powder diffraction, IR and NMR spectroscopy, and methanol sorption measurements. The chemical composition of the bulk starting material was $(\text{NH}_4)_{10.6}\text{Cs}_{0.7}\text{Al}_{11.3}\text{Si}_{36.7}\text{O}_{96}\cdot 43\text{H}_2\text{O}$. After calcination at 773 K, deuteration and dehydration the chemical composition of the dealuminated framework with its exchangeable cations was $\text{D}_{5.3}\text{Cs}_{0.7}\text{Al}_6\text{Si}_{42}\text{O}_{96}$. After partial rehydration the approximate chemical composition was $\text{D}_{5.3}\text{Cs}_{0.7}\text{Al}_6\text{Si}_{42}\text{O}_{96}\cdot 30\text{D}_2\text{O}$, $M_r = 3582.26$, centrosymmetric space group $Im\bar{3}m$, $a = 15.0387(5) \text{ \AA}$, $V = 3401.2 \text{ \AA}^3$, $D_x = 1.748 \text{ g cm}^{-3}$, $R_{wp} = 5.1\%$. At room temperature the dehydrated zeolite ($M_r = 2981.37$) is noncentrosymmetric (space group $I\bar{4}3m$) with $a = 14.8803(4) \text{ \AA}$, $V = 3294.8 \text{ \AA}^3$, $D_x = 1.502 \text{ g cm}^{-3}$, $R_{wp} = 4.7\%$. At 623 K it is centrosymmetric ($Im\bar{3}m$) with $a = 15.0620(3) \text{ \AA}$, $V = 3417.0 \text{ \AA}^3$, $D_x = 1.448 \text{ g cm}^{-3}$, $R_{wp} = 3.7\%$. The structure analysis based on neutron powder diffraction data reveals in all three cases the presence of a bridging hydroxyl group, with O–D distances ranging from 0.96 to 1.01 Å, and approximate planarity of the two adjoining T (=Si,Al) sites, the bridging O atom and the D atom. Ammonia desorption studies show the OH group in H-Rho to be weakly acidic; thus, this represents the first known example of a

weakly acidic, bridging hydroxyl group in a zeolite. Near the single six-membered ring of the aluminosilicate framework an Al–O group has been located, in which the nonframework Al atom is in a very distorted tetrahedral coordination. The overall charge of the species must be neutral, because charge balance is obtained by D atoms attached to the bridging framework O atoms. The Al–O group is either AlO^+ charge-balanced by an equal number of AlO_2^- moieties or is part of a neutral Al_2O_3 group.

Introduction

When the NH_4^+ form of a silica-rich zeolite is calcined at temperatures between about 700 and 1000 K, a highly acidic hydrogen form of the zeolite is usually obtained. At the same time, the tetrahedral aluminosilicate framework TO_2 of the zeolite, where T is (Si,Al), is partly dealuminated (Kerr, 1973). The resultant H-zeolites have increased catalytic activity (Flockhart, Megarry & Pink, 1973), perhaps related to non-framework aluminium (NFA). On the basis of quantum chemical studies the H atoms are assumed to reside in hydroxyl groups, either bridging between Al and Si, or in terminal hydroxyl groups in defect positions of the framework (Mortier, Sauer, Lercher & Noller, 1984; Geerlings, Tariel, Botrel, Lissillour & Mortier, 1984). Direct experimental diffraction evidence for the location of the H atoms is tentative. Neither Jiráček, Vratislav & Bosáček (1980) nor Cheetham, Eddy & Thomas (1984) in their studies of H-containing zeolite Y could establish the positions of the H atoms beyond reasonable doubt.

* Present address: Mineralogisches Institut der Universität, Am Hubland, D-8700 Würzburg, Federal Republic of Germany.

† Contribution No. 4109.

The NFA has been reported to reside in the sodalite cages of zeolite A (Pluth & Smith, 1982) and in both the supercages and sodalite cages of zeolite Y (Maher, Hunter & Scherzer, 1971; Parise, Corbin, Abrams & Cox, 1984; Shannon, Gardner, Staley, Bergeret, Gallezot & Auroux, 1985, and references therein).

We have been especially interested in zeolite dehydroxylation and dealumination processes with the specific goals of finding the D atoms of the framework hydroxyl groups and the nonframework Al species by using neutron diffraction methods, magic-angle-spinning nuclear magnetic resonance (MAS NMR) spectroscopy and infrared spectroscopy. Upon calcination zeolites NH₄-Rho and NH₄-ZK-5 undergo deammoniation, some dehydroxylation and partial extraction of aluminium from the (Si,Al)O₂ framework. The first two papers in this series (Fischer, Baur, Shannon, Staley, Vega, Abrams & Prince, 1986*a,b*) dealt with deep-bed-calcined Rho and ZK-5 which suffered extensive dealumination. The crystal structure refinements of the deep-bed samples gave an indication of the presence of randomly distributed, nonframework, condensed aluminium oxide or hydroxide species. The third paper (Baur, Fischer, Shannon, Staley, Vega, Abrams, Corbin & Jorgensen, 1987) described D-Rho calcined under dry shallow-bed conditions where relatively little framework dealumination occurred. Although bridging hydroxyl groups with a stretching frequency of 3610 cm⁻¹ were found, the two to four NFA atoms found by NMR measurements were not located.

Shallow-bed calcination of H-Rho under 81.5 kPa H₂O results in removal of ~50% of the framework Al and the formation of hydroxyl groups with a stretching frequency of 3640 cm⁻¹, suggesting the generation of a homogeneous population of framework hydroxyls different from those of dry, shallow-bed-calcined H-Rho. Ammonia desorption further shows that the acidity of the 3640 cm⁻¹ hydroxyls is substantially lower than that of the 3610 cm⁻¹ species. H-Rho samples with a sharp 3640 cm⁻¹ band thus afford an opportunity to identify the NFA structure since such Al may be expected to exist in a relatively homogeneous population of sites in these samples. Results on the centrosymmetric, high-temperature form of D-Rho-SS773 (D_{5.3}Cs_{0.7}Al₆Si₄₂O₉₆) have been reported previously (Fischer, Baur, Shannon & Staley, 1987). D atoms attached to O in bridging framework positions could be located and successfully refined. A non-framework aluminium oxygen group was found close to the six-membered rings of (Si,Al)O₄ tetrahedra in the *a* cage. This paper contains the full information and interpretation of the physicochemical properties of the sample, as well as further data on the zeolite in its noncentrosymmetric and its hydrated form. Sample designations are explained in Fischer *et al.* (1986*a*). They include both the calcination temperature and the

data-collection temperature in K, separated by a slash. SS refers to shallow-bed calcination in steam.

Experimental

Na,Cs-Rho was prepared according to the method described by Robson, Shoemaker, Ogilvie & Manor (1973) and Fischer *et al.* (1986*a*). The initial gel was allowed to stand for 5 days at room temperature and heated at 373 K for 6 days. The product was exchanged four times in 10% NH₄NO₃ solution to yield (NH₄)_{10.6}Na_{0.02}Cs_{0.70}Al_{11.3}Si_{36.7}O₉₆ as determined by wet chemical analysis (Si/Al = 3.2). Scanning electron micrographs showed dodecahedral crystals of zeolite Rho, ~0.5 μm in diameter, and of spherical chabazite aggregates (~10 vol.%) of similar size. H-Rho-SS773 was prepared by heating NH₄-Rho to 773 K for 1 h under rapidly flowing N₂ (1000 cm³ min⁻¹) to produce H-Rho and then maintaining the sample at 773 K for 4 h under 1000 cm³ min⁻¹ N₂ equilibrated to provide 81.5 kPa H₂O. X-ray diffraction patterns showed that the chabazite impurity phase had been rendered amorphous during the initial conversion to H-Rho. A mid-infrared spectrum showed a T—O stretching frequency of 1070 cm⁻¹, which when compared to 1060 cm⁻¹ for H-Rho-S873 indicated considerable framework dealumination.

The samples were dehydrated overnight at 633 K, subsequently deuterium exchanged in seven cycles of exposure to D₂O at 553 K for about 15 min and dehydrated at 633 K for about 30 min. The exchange was completed by two final cycles of approximately 1 h each at room temperature to give D_{5.3}Cs_{0.7}Al₆Si₄₂O₉₆ (D-Rho-SS773) with ~5 Al atoms outside of the framework. An infrared scan of the dehydrated sample showed no water remaining and no protons were detected by ¹H NMR. Part of the sample which was deuterated in a similar way was exposed to an amount of D₂O calculated to give 30 molecules of D₂O per unit cell. Dehydrated and hydrated samples were loaded into vanadium cans for the neutron diffraction experiments and sealed with an indium o-ring in a dry nitrogen atmosphere. The o-ring melted at 430 K and exposed the sample to the vacuum of the sample chamber. It is unlikely that at 623 K the sample could have adsorbed any molecules in the vacuum chamber. Sorption measurements were carried out as described in Fischer *et al.* (1986*a,b*).

Infrared experiments were performed with a Nicolet 3600 FTIR spectrometer. The samples were kept in air for a long period before the infrared experiments were carried out so that all deuterium was removed by exchange with atmospheric water vapor. Sample pellets (10 mg) of 1.0 cm diameter were mounted in the spectrometer in an all-metal vacuum system having a base pressure <1.3 × 10⁻⁶ Pa. The samples were contained, inside the vacuum system, in a quartz oven

Table 1. *Experimental conditions, crystallographic data and definitions used in data refinement*

Standard deviations are given in parentheses. The approximate chemical composition of the samples is $D_{5.5}C_{80.7}Al_6Si_{42}O_{96}$ for D-Rho-SS773/RT and D-Rho-SS773/623, and $D_{5.5}C_{80.7}Al_6Si_{42}O_{96} \cdot 30D_2O$ for D-Rho/W-SS773/RT (this excludes the nonframework aluminium species).

	D-Rho-SS773/RT	D-Rho-SS773/623	D-Rho/W-SS773/RT
Neutron flight path (m)	15.5	15.5	15.5
Detector position (°)	±90	±90	±90
Sample container	Vanadium can of ~ 11.3 mm diameter		
Interval between consecutive profile points (μs)	7	7	7
Space group	$I43m$	$Im\bar{3}m$	$Im\bar{3}m$
Formula weight (dalton)	2981.37	2981.37	3582.26
D_x (g cm ⁻³)	1.502	1.448	1.748
V (Å ³)	3294.8	3417.0	3401.2
Data collection temp. (K)	RT	623	RT
Calcination temp. (K)	773	773	773
Cell constants, a (Å)	14.8803 (4)	15.0620 (3)	15.0387 (5)
Range of d values (Å)	0.96–5.37	0.95–5.37	1.00–5.37
$(d/\sigma)_{max}$	0.22	0.08	0.11
No. of observations	2734	2256	2661
No. of reflections	243	251	217
No. of variable profile parameters	7	8	8
No. of variable structure parameters*	26	22	14
R_{wp} (%)	4.7	3.7	5.1
R_p (%)	2.3	1.9	1.6
R_I (%)	8.5	9.4	13.3
R_p (%)	3.1	2.4	2.9
Definitions†	$R_{wp} = \left[\frac{\sum_i w_i (y_{oi} - 1/Cy_{ci})^2}{\sum_i w_i y_{oi}^2} \right]^{1/2}$ $R_p = \left[\frac{1}{(N-P)} \sum_i w_i y_{oi}^2 \right]^{1/2}$ $R_I = \frac{\sum_i I_{oi} - 1/Cy_{ci} }{\sum_i I_{oi}}$ $R_p = \frac{\sum_i y_{oi} - 1/Cy_{ci} }{\sum_i y_{oi}}$ $w = 1/y_{oi}$		

* Including scale factor.

† R_{wp} = weighted residual including profile intensities; R_p = unweighted profile residual; R_p = statistically expected residual; R_I = residual including integrated intensities; N = No. of statistically independent observations; P = No. of variable least-squares parameters; y_{oi}, y_{ci} = observed and calculated profile intensities; I_{oi}, I_{ci} = observed and calculated integrated intensities; C = scale factor. Residuals and refinement are based on data points in the profile which have an intensity greater than 0.01 of the corresponding maximum peak intensity.

capable of heating the sample to 973 K. The ammonia desorption experiments were performed by dosing the samples, previously heated under vacuum at 723 K, with 133.3 Pa ammonia at constant pressure at 323 K and then heating for 10 min at 323 to 723 K in steps of 50 K. Spectra were taken at 323 K following each heating step.

The solid-state NMR experiments were performed with a Bruker CXP-300 spectrometer. After completion of the diffraction experiments the deuterated samples were protonated by several cycles of exposure to H₂O vapors and evacuation at 623 K. The resulting hydrogen contents were determined by proton spin counting and the proton magic-angle-spinning (MAS) spectra were also obtained under anhydrous conditions. Prior to the ²⁹Si and quantitative ²⁷Al MAS measurements the samples were rehydrated over a saturated ammonium chloride solution. All NMR measurements were performed at room temperature. Further experimental details are as previously reported (Fischer *et al.*, 1986a; Vega & Luz, 1987).

The time-of-flight neutron diffraction data were collected on the Special Environment Powder Diffractometer at the Intense Pulsed Neutron Source of Argonne National Laboratory (Jorgensen & Faber, 1983). Experimental conditions, crystallographic data and basic equations and definitions are given in Table 1. The structure refinements were performed with a local version (Rotella, 1982) of Rietveld's (1969) program adapted to the time-of-flight method by Von Dreele, Jorgensen & Windsor (1982). The coherent neutron scattering lengths used in the refinements are $b(\text{Si}) = 4.1491$, $b(\text{Al}) = 3.449$, $b(\text{O}) = 5.803$, $b(\text{D}) = 6.67$ and $b(\text{Cs}) = 5.42$ fm (Koester, 1977). The scattering length of the Si and Al atoms occupying statistically the tetrahedral site T was calculated by linear interpolation according to the Si/Al ratio determined by MAS NMR spectroscopy.

Interatomic distances and angles were calculated with the program *SADIAN86* (Baur, Wenninger & Roy, 1986), the crystal structure illustrations were drawn with the plot program *STRUPLO84* (Fischer, 1985).

Results

Sorption

Methanol sorption was 21.3 g/100 g sample for D-Rho-SS773. Methanol sorption results for Rho samples under various conditions have shown an upper limit of ~24.0 g/100 g sample. This limit is presumably obtained for the fully accessible Rho structure. The methanol sorption results for D-Rho-SS773 thus indicate a structure in which the pores are ~89% accessible.

Infrared spectroscopy

Infrared studies were carried out on H-Rho-SS773 and, for comparison, an NH₄-Rho similar to that used to prepare D-Rho-SS773. All samples were heated under vacuum in the infrared spectrometer at 723 K. In the case of the NH₄-Rho precursor, these mild calcination conditions give a relatively pure H-Rho. H-Rho-SS773 was free of ammonia as indicated by the absence of the NH-bending feature at 1450 cm⁻¹. A spectrum of the hydroxyl-stretching features of H-Rho-SS773 is shown in Fig. 1. The area under the features from 3500 to 3700 cm⁻¹ gives an approximate measurement of the internal hydroxyl content of the sample. The hydroxyl content of H-Rho-SS773 is reduced, compared to the vacuum-calcined precursor, to about 50%. The position of the hydroxyl feature is also altered. In the vacuum-calcined precursor the main feature is at 3610 cm⁻¹; in H-Rho-SS773 it appears at 3640 cm⁻¹ (Fig. 1). Ammonia chemisorbed by H-Rho-SS773 at 373 K is only about 50% of that chemisorbed by H-Rho-S773, and is substantially

desorbed on heating at 423 K for H-Rho-SS773 compared to 623 K for H-Rho-S773.

Nuclear magnetic resonance spectroscopy

The quantitative proton NMR measurements gave a hydrogen concentration of 7 ± 1 atoms per unit cell. Quantitative information on the state of the aluminium was obtained from the ^{29}Si and ^{27}Al MAS NMR measurements on the rehydrated sample, the spectra of which are shown in Fig. 2 together with the proton MAS spectrum of the anhydrous sample. The ^{29}Si lineshape consists of three peaks at -99 , -104 and

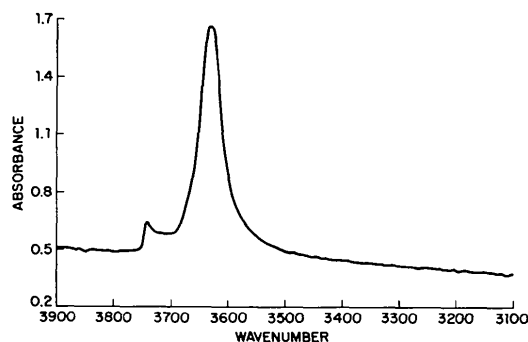


Fig. 1. Hydroxyl-stretching region of the infrared spectra of H-Rho-SS773.

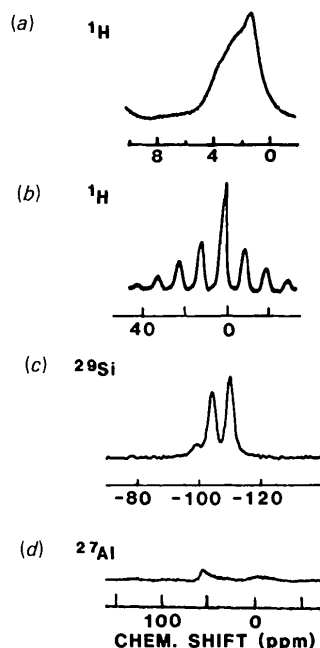


Fig. 2. Magic-angle-spinning NMR spectra of D-Rho-SS773. (a) Proton spectra of the protonated, anhydrous sample; (b) the expanded centerband region and the full spectral width showing the sideband pattern. The spinning rate was 3 kHz. The spectra were obtained with single 90° radio-frequency pulses. (c) ^{29}Si spectrum. (d) ^{27}Al spectrum of the rehydrated sample, obtained with single 15° pulses.

-110 p.p.m., corresponding to Si atoms linked to 2, 1 and 0 Al atoms, respectively. From the relative peak intensities (8:41:51) we derived a framework Si:Al ratio of 7.0 (Klinowski, 1984), a clear indication of extensive dealumination.

The quantitative ^{27}Al measurement showed that only 1.3 atoms per unit cell contributed to the ^{27}Al MAS lineshape shown in Fig. 2. Of these, about 0.8 contribute to the tetrahedral Al peak at 59 p.p.m. and 0.5 to the octahedral peak. On the other hand, almost 90% of the Al sites are not directly detected in the MAS spectrum, indicating that their site symmetry deviates substantially from tetrahedral or octahedral symmetry, even in the hydrated state. In this respect the present Rho sample differs from the vacuum-calcined (Vega & Luz, 1987) and shallow-bed-calcined forms of H-Rho (Baur *et al.*, 1987), where essentially all the Al sites are in symmetric sites.

The most significant NMR result is the chemical shift of the protons. In the top trace of Fig. 2 we see a small peak at a somewhat higher field. The second trace, representing a wider spectral range of the proton MAS spectrum, shows that only the dominant center peak is accompanied by spinning sidebands. From the sideband positions we find by interpolation that the main center peak resonates at 2.1 p.p.m. As usual, we assign the signal at 1.2 p.p.m. to terminal hydroxyl groups. They correspond to about 3% of the total proton count and probably come from the amorphitized chabazite or from terminal OH groups formed at defects in the slightly dealuminated H-Rho. From the NMR data alone we cannot identify the nature of the 2.1 p.p.m. H atoms, as we have no precedent for such a chemical shift of the dominant peak in an H-zeolite spectrum. In accordance with the infrared data, it appears to result from a single uniform H species. One notices that the sidebands are stronger than those usually observed for bridging hydroxyl groups in zeolites (Vega & Luz, 1987; Baur *et al.*, 1987). We also found that the nonspinning proton spectrum is 8.1 kHz, *i.e.* 15% wider than the corresponding spectrum of shallow-bed-calcined Rho. These observations suggest that the ^1H - ^{27}Al dipolar interaction is stronger than in the bridging OH group of shallow-bed-calcined Rho, presumably because the Al-H distance is shorter. Since the dipolar broadening is proportional to the cube of the Al-H distance, we may estimate that this distance is 5% shorter in the hydrothermally treated form of H-Rho. However, other interpretations, such as differences in proton mobility or ^1H - ^1H homonuclear interactions, could be considered as possible sources for the differences in sideband intensities.

Rietveld analysis and structure refinement

Data for dehydrated Rho were collected at room temperature (D-Rho-SS773/RT) and at 623 K (D-

Rho-SS773/623), while the hydrated sample (D-Rho/W-SS773/RT) was examined at room temperature only. Irregularly increased background, apparently resulting from the amorphitized chabazite, was corrected by the polynomial fitting method as described by Baur & Fischer (1986).

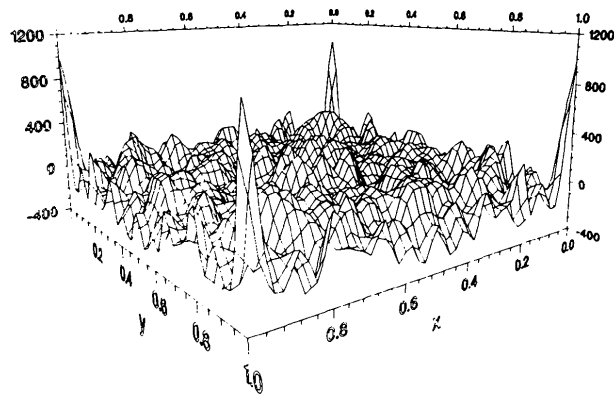
The refinement of the crystal structure including only framework atoms showed it to be noncentrosymmetric at room temperature and centrosymmetric at 623 K. Subsequent Fourier and difference Fourier syntheses did not give any evidence for possible nonframework positions. The strongest peak in the difference map of the high-temperature form was in 0,0,0 as shown in Fig. 3(a). The occupancy of an atom in this position, to which the scattering length of aluminium had been assigned, was refined to about one atom per unit cell. This position has zero coordination to the framework atoms and is therefore unlikely for any nonframework

The grid-search method (Baur & Fischer, 1986) immediately revealed the deuterium position in the centrosymmetric structure (Fischer *et al.*, 1987). For each of the positions of a grid with a step size of 0.3 Å the occupancy of a dummy atom was refined in the asymmetric unit and the results plotted in layers of the unit cell. A plot of the *xy* layer corresponding to a layer of the difference map is given in Fig. 3(b). It can clearly be seen that there is no evidence for scattering around 0,0,0. However, eight symmetrically related peaks occur in an *xy*0 position with approximate coordinates of $x = 0.40$ and $y = 0.14$ at a distance of about 1.2 Å from framework atom O(1). It was therefore assigned to deuterium. The final refinement of the positional coordinates yielded an interatomic distance O(1)–D of 0.96 (2) Å thus confirming this assignment. Similar results were obtained for D-Rho-SS773/RT and D-Rho/W-SS773/RT. The occupancy factors of the D positions in the three refined structures range from seven to twelve D atoms per unit cell. The value of twelve D atoms per unit cell, which is too high, is for the hydrated sample (D-Rho/W-SS773/RT) where no nonframework positions other than deuterium could be refined. Only six D atoms are needed to balance the charge on the framework, since according to the NMR analysis six of the 48 tetrahedral framework atoms per unit cell are occupied by aluminium. Also the ¹H NMR shows only seven H atoms per unit cell in an H-Rho with identical composition.

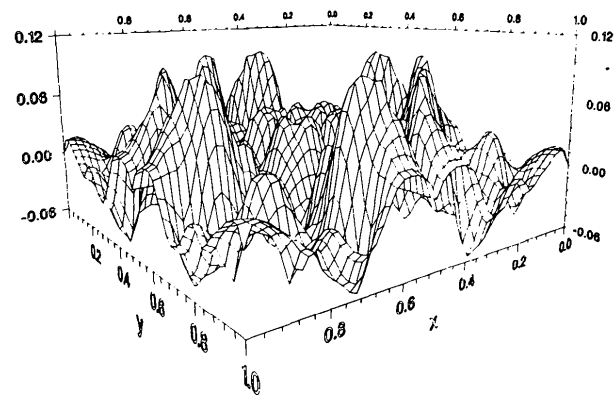
The search map showed six more peaks, four of them close to the center of the single six-membered ring (6R) and two close to the center of the double eight-membered ring (D8R). We interpreted these peaks on the basis of the following assumptions:

(a) each of these positions is occupied by only one atom species, that is either oxygen or aluminium;

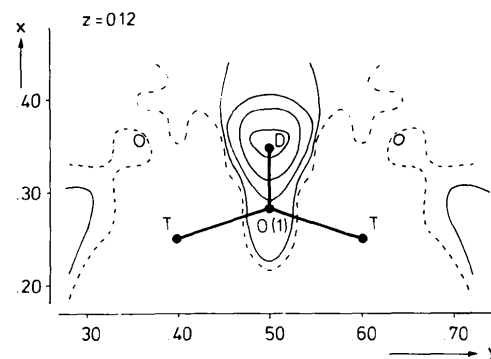
(b) each of the nonframework atoms is bonded to the framework by a strong, short bond, not by a long hydrogen bond;



(a)



(b)



(c)

Fig. 3. (a) An *xy* layer of a difference Fourier map of D-Rho-SS773/623 for $z = 0$. Heights are in arbitrary units. (b) The corresponding *xy* layer in the grid-search map. Heights refer to occupancy factors of a dummy atom. Peaks in the two maps usually do not coincide. Peaks found in the grid search have a high probability of remaining stable in subsequent Rietveld refinements. (c) The highest peak in the grid-search map assigned to deuterium. Each line corresponds to 2.0 D atoms per unit cell. The zero line is dot-dashed. Framework *T* sites and oxygen positions are indicated. These sites were held fixed in the grid-search procedure. The *T*–OD–*T* configuration represents an almost ideal planar geometry.

(c) the lengths of these bonds must be within a few e.s.d.'s of the bond lengths estimated from the sum of their effective ionic radii (Shannon, 1976);

(d) the overall formal charge of the nonframework species must be zero, because charge balance is already attained by the deuterium ions;

(e) the nonframework species cannot contain OD groups, because ^1H NMR of an H-Rho similar to the D-Rho described here shows that there are no more H atoms in D-Rho than already located in the D sites.

On the basis of these criteria only two of the peaks close to the six-membered ring were acceptable and remained stable in the refinements. One position refined to a distance of 1.92 (5) Å to O(2) and was assigned to aluminium [Al(nf)]. Another position was assigned to a nonframework O atom [O(nf)] at a distance of 1.61 (5) Å from Al(nf).

The occupancies of the nonframework aluminium and oxygen are higher than for caesium (five to eight atoms per unit cell), but still small enough to be tentative in terms of their actual values. This is especially true because occupancy factors and thermal parameters for these positions are strongly correlated, presumably because the background problems did not allow us to extend the refinement to even smaller d values. However, the occupancies are within the limits given by the symmetry restrictions of the space groups. Owing to the proximity of the nonframework species to the threefold axes only one third of the atoms in position 24(g) in $I\bar{4}3m$ can be occupied in any given single six-membered ring. The refinement yielded 8.0 (5) atoms per unit cell which is in perfect agreement with these restrictions. The temperature factors were held constant at 5 Å². It is reasonable in the case of zeolites to assume that the temperature factors of the nonframework positions are larger than those of atoms in the framework (those varied from 0.5 to 3.0 Å²). In the only case where the temperature factor of a nonframework atom could be refined simultaneously with its occupancy (the D atom in D-Rho/W-SS773/RT) it yielded a value of 5.1 (9) Å². In order to test the sensitivity of the choice of B on the occupancy factor in cases where B had to be held constant, we varied the temperature factor of one nonframework atom systematically from 1 to 10 Å². The simultaneously refined occupancy was twice as high for $B = 10$ Å² as for $B = 1$ Å². With each increase of 1 Å² the occupancy factor was raised by about 8%. Both the positional coordinates and the occupancy factors of the nonframework positions are heavily affected by the presence or absence of other atoms in the refinement. This is similar to what was observed for the interatomic distances $T\text{—O}$, except the effects are more pronounced. There are about 0.7 Cs atoms in the unit cell according to the chemical analysis. A refinement of a Cs atom in Wyckoff site 12(e) converged to $x = 0.452$ (4) with 1.7 atoms per unit cell. This site has

Table 2. R_1 and R_{wp} values, number of negative temperature factors and mean (Si,Al)—O distances (Å) (with the mean e.s.d.'s of the individual (Si,Al)—O distances) at three different stages of the refinement

Cut-offs at low values, profile parameters and cell constants are identical at each of the three stages of refinement reported here. Therefore, the differences in R values reflect only the improvements owing to the polynomial fitting of the background and the inclusion of the nonframework atoms.

Sample	Status	R_1	R_{wp}	No. of negative temp. factors	(Si,Al)—O distances
D-Rho-SS773/RT	Standard background correction, framework atoms refined	15.3	7.4	4 of 4	1.642 (9)
	Polynomial fitting of background, framework refined	9.4	5.4	0	1.637 (8)
	Same as above, nonframework atoms refined	8.5	4.7	0	1.632 (7)
D-Rho-SS773/623	Standard background correction, framework atoms refined	23.3	8.7	1 of 3	1.635 (7)
	Polynomial fitting of background, framework refined	11.6	4.6	0	1.632 (8)
	Same as above, nonframework atoms refined	9.4	3.7	0	1.625 (5)
D-Rho/W-SS773/RT	Standard background correction, framework atoms refined	26.0	7.6	2 of 3	1.640 (7)
	Polynomial fitting of background, framework refined	17.0	5.6	0	1.626 (8)
	Same as above, nonframework atoms refined	13.3	5.1	0	1.624 (6)

been found to be occupied by Cs in previous refinements of zeolite Rho.

The grid-search method was also applied to the low-temperature form and yielded positions similar to the high-temperature form, except that the Cs-atom position was not stable in the refinements. In the hydrated form only the deuterium position could be identified. There was no indication of the presence of any well resolved D₂O molecules or for any nonframework aluminium species.

The significant improvement of the results obtained by polynomial fitting of the background and by inclusion of the nonframework positions in the refinements is shown in Table 2. Before the background correction seven out of ten framework atoms had negative isotropic temperature factors, after the correction the temperature factors had normal values. In D-Rho-SS773/623 and in D-Rho/W-SS773/RT the isotropic temperature factors and the occupancy factors of the D atoms could be varied simultaneously and the O(1)—D distances refined to the values expected for an O—H distance. The refined atomic parameters are listed in Table 3, a selection of

Table 3. *Positional parameters in fractional coordinates, isotropic temperature factors (\AA^2), site symmetry, Wyckoff positions and occupancies*

	<i>x</i>	<i>y</i>	<i>z</i>	<i>B</i>	Site symmetry*	Wyckoff position*	No. of atoms in unit cell
(a) D-Rho-SS773/RT							
Si/Al(<i>T</i>)	0.2640 (4)	0.1170 (4)	0.4117 (4)	1.5 (1)	1	48 (<i>h</i>)	42/6†
O(1)	0.0201 (2)	0.2139 (3)	0.3873 (3)	0.9 (1)	1	48 (<i>h</i>)	48
O(2)	0.1971 (3)	<i>x</i>	0.3856 (5)	1.5 (1)	.. <i>m</i>	24 (<i>g</i>)	24
O(3)	0.1416 (2)	<i>x</i>	0.6257 (3)	0.8 (1)	.. <i>m</i>	24 (<i>g</i>)	24
D	0.029 (2)	0.147 (3)	0.393 (2)	5.0‡	1	48 (<i>h</i>)	6.9 (5)
Al(nf)	0.267 (2)	<i>x</i>	0.313 (3)	5.0‡	.. <i>m</i>	24 (<i>g</i>)	8.0 (5)
O(nf)	0.328 (2)	<i>x</i>	0.388 (3)	5.0‡	.. <i>m</i>	24 (<i>g</i>)	4.6 (3)
(b) D-Rho-SS773/623							
Si/Al(<i>T</i>)	$\frac{1}{2}$	0.1029 (2)	$\frac{1}{2}-y$	1.0 (1)	..2	48 (<i>i</i>)	42/6†
O(1)	0	0.2173 (3)	0.3841 (2)	2.5 (1)	<i>m</i> ..	48 (<i>j</i>)	48
O(2)	0.1667 (2)	<i>x</i>	0.3760 (2)	2.9 (1)	.. <i>m</i>	48 (<i>k</i>)	48
D	0	0.381 (1)	0.154 (1)	3.8 (7)	<i>m</i> ..	48 (<i>j</i>)	8.4 (5)
Cs	0.452 (4)	0	0	5.0‡	4 <i>m.m</i>	12 (<i>e</i>)	1.7 (2)
Al(nf)	0.208 (2)	<i>x</i>	0.263 (4)	5.0‡	.. <i>m</i>	48 (<i>k</i>)	5.5 (4)
O(nf)	0.303 (1)	<i>x</i>	0.375 (2)	5.0‡	.. <i>m</i>	48 (<i>k</i>)	4.9 (3)
(c) D-Rho/W-SS773/RT							
Si/Al(<i>T</i>)	$\frac{1}{2}$	0.1026 (3)	$\frac{1}{2}-y$	0.5 (1)	..2	48 (<i>i</i>)	42/6†
O(1)	0	0.2182 (4)	0.3838 (3)	1.2 (1)	<i>m</i> ..	48 (<i>j</i>)	48
O(2)	0.1681 (2)	<i>x</i>	0.3728 (3)	3.0 (1)	.. <i>m</i>	48 (<i>k</i>)	48
D	0	0.397 (1)	0.154 (2)	5.1 (9)	<i>m</i> ..	48 (<i>j</i>)	12.0 (9)

* After *International Tables for Crystallography* (1983).

† Si/Al ratio from MAS NMR.

‡ Held constant in refinement.

interatomic distances is given in Table 4. Observed and calculated powder patterns are shown in Figs. 4 and 5.*

Discussion

Phase transition

Parise, Gier, Corbin & Cox (1984) predicted that zeolites Rho with unit-cell constants greater than 14.95 Å should crystallize in the centrosymmetric space group $Im\bar{3}m$, while those with smaller cell constants should be noncentrosymmetric in space group $I\bar{4}3m$. The change in cell constants and symmetry was observed to occur when zeolite Rho was undergoing drastic changes in chemical composition upon hydration/dehydration (McCusker & Baerlocher, 1984; Parise, Gier *et al.*, 1984) or upon variation in calcination temperature (McCusker, 1984; Fischer *et al.*, 1986a). Increasing calcination temperatures result in increasing Si/Al ratios. In our case the sample was already dehydrated and it had been calcined previously. The change from noncentrosymmetric to centrosymmetric occurred when we heated the sample from room temperature to 623 K in the vanadium can in the diffractometer. During diffraction data collection we did not realize that a phase transition had taken place and therefore we did not check for reversibility.

* Lists of numerical values corresponding to the data in Figs. 4 and 5, and observed and calculated intensities for D-Rho/W-SS773/RT have been deposited with the British Library Document Supply Centre as Supplementary Publication No. SUP 44920 (44 pp.). Copies may be obtained through The Executive Secretary, International Union of Crystallography, 5 Abbey Square, Chester CH1 2HU, England.

Table 4. *Selected interatomic distances (Å) and angles (°)*

(a) D-Rho-SS773/RT			
Si/Al—O(2)	1.601 (8)	O(1)—O(1)	2.638 (6)
Si/Al—O(3)	1.618 (7)	O(1)—O(3)	2.643 (5)
Si/Al—O(1)	1.647 (7)	O(1)—O(2)	2.646 (5)
Si/Al—O(1)	1.663 (7)	O(2)—O(3)	2.656 (5)
Mean	1.632 (7)	O(1)—O(3)	2.698 (5)
Estimated mean	1.623 (see text)	O(1)—O(2)	2.709 (6)
Al(nf)—O(nf)	1.70 (5)	O(nf)—Al(nf)—O(2)†	103 (3)
Al(nf)—O(2)	1.83 (4)	O(nf)—Al(nf)—O(3)	89 (1) (×2)
Al(nf)—O(3)	2.59 (3) (×2)	O(2)—Al(nf)—O(3)	72 (1) (×2)
Al(nf)—Si/Al	2.67 (4) (×2)	O(3)—Al(nf)—O(3)	141 (1)
Al(nf)—O(2)	2.68 (4) (×2)	Si/Al—O(2)—Si/Al	150.1 (6)
O(nf)—O(2)	2.75 (3)	Si/Al—O(3)—Si/Al	147.6 (4)
O(nf)—O(3)	3.08 (3) (×2)	Si/Al—O(1)—Si/Al	140.2 (4)
		Si/Al—O(1)—D	109.2 (17)
		Si/Al—O(1)—D	108.1 (17)
		Sum of angles around O(1)	357.5
(b) D-Rho-SS773/623			
Si/Al—O(2)	1.612 (4) (×2)	O(1)—O(2)	2.627 (3)
Si/Al—O(1)	1.638 (5) (×2)	O(1)—O(1)	2.658 (4)
Mean	1.625 (4)	O(2)—O(2)	2.669 (4)
Estimated mean	1.622 (see text)	O(1)—O(2)	2.670 (4)
Al(nf)—O(nf)	1.61 (5)	O(nf)—Al(nf)—O(2)	105 (2)
Al(nf)—O(2)	1.92 (6)	O(nf)—Al(nf)—O(2)	143 (2)
Al(nf)—O(2)	2.51 (4) (×2)	O(nf)—Al(nf)—O(2)	87 (2)
Al(nf)—Si/Al	2.64 (5) (×2)	O(2)—Al(nf)—O(2)	73 (1) (×2)
Al(nf)—O(2)	2.98 (4) (×2)	O(2)—Al(nf)—O(2)	126 (2)
O(nf)—O(2)	2.81 (2) (×2)	Si/Al—O(2)—Si/Al	152.8 (3)
O(nf)—O(2)	2.90 (2)	Si/Al—O(1)—Si/Al	142.2 (3)
Cs—O(1)	3.43 (2) (×4)	Si/Al—O(1)—D	107.8 (2) (×2)
Cs—O(2)	3.73 (2) (×4)		
Cs—O(1)	4.10 (4) (×4)	Sum of angles around O(1)	357.8
(c) D-Rho/W-SS773/RT			
Si/Al—O(2)	1.620 (5) (×2)	O(1)—O(2)	2.643 (4)
Si/Al—O(1)	1.628 (7) (×2)	O(1)—O(1)	2.650 (5)
Mean	1.624 (6)	O(2)—O(2)	2.612 (4)
Estimated mean	1.622 (see text)	O(1)—O(2)	2.682 (5)
Si/Al—O(2)—Si/Al	150.8 (4)		
Si/Al—O(1)—Si/Al	142.7 (4)		
Si/Al—O(1)—D	105.2 (4) (×2)		
		Sum of angles around O(1)	353.1

Whatever chemical change took place during heating to 623 K must have been minor compared to the changes upon calcination to 773 K or upon hydration.

The increase in the cell constant from the non-centrosymmetric D-Rho-SS773/RT (14.880 Å) to the centrosymmetric phase at 623 K (15.062 Å) is 0.18 Å or 1.2%. This gives an indication how flexible the framework of this zeolite is. The increase is mostly due to the opening up by about 4° of the $T-O(2)-T$ angle in D-Rho-SS773/623 as compared with D-Rho-SS773/RT (Table 4). Interestingly, the addition of water to D-Rho-SS773 gave a cell constant 0.02 Å smaller than in D-Rho-SS773/623 but it stayed centrosymmetric

Table 5. Summary of results from physical and chemical characterization of D-Rho-SS773 and the precursor NH_4 -Rho

Quantity	Method	NH_4 -Rho	D-Rho-SS773
Al(fr) (per unit cell)	^{29}Si NMR	12	6 ^a
	^{27}Al NMR	12 ^a	0.8 ^a
Al(nf) (per unit cell)	^{29}Si NMR	—	6 ^a
	^{27}Al NMR	—	0.5 ^a
	Neutron diffraction	—	6.8 (5)
H ⁺ (per unit cell)	1H NMR	45	7
MeOH capacity (relative)	Sorption	100%	89%

Notes: (a) Samples rehydrated over saturated ammonium chloride solution. (b) The difference between ^{29}Si NMR results before and after calcination. (c) In protonated, dehydrated samples. (d) The estimated error is 10%. Chemical analysis indicates ~11 Al atoms per unit cell.

while $T-O(2)-T$ was reduced by 2° relative to the dehydrated form.

Sorption, infrared and NMR spectroscopy

The sorption, infrared spectroscopy and nuclear magnetic resonance spectroscopy results provide a chemical characterization of the samples which is useful in understanding the structural results.

Shallow-bed calcination in the presence of steam results in extensive dealumination of the zeolite framework. Many of the 11 Al atoms per unit cell originally in the framework of these zeolites are not observed by ^{29}Si or ^{27}Al NMR in hydrated D-Rho after calcination (Table 5). The Al per unit cell value from the ^{29}Si NMR results (Table 5) shows that only about 55% of the Al atoms remain associated with framework Si atoms in D-Rho/W-SS773. The Al per unit cell value from ^{27}Al NMR is even lower, 7% for D-Rho-SS773. Most of the remaining Al atoms in hydrated D-Rho are in sites where the local symmetry is so greatly distorted that the ^{27}Al peaks are broadened to the point that they are not observable. The magnitude of the electric quadrupolar interaction constant increases with the geometric deviation from tetrahedral symmetry, causing this effect (Ghose & Tsang, 1973).

The NMR results clearly indicate an extensive dealumination of the framework. They do not give direct information on the dealumination process, but the following models have been considered:

(a) The vacancies created at the dealuminated T sites are filled by Si atoms that have migrated from other regions of the zeolite. The total number of T sites is then 48 and an Si:Al ratio of seven corresponds to six framework Al atoms per unit cell.

(b) The aluminosilicate framework could also be restored by a rearrangement of Si—O—Si linkages, without long-range migration of atomic species. In that case the number of Si atoms per unit cell remains equal to that before the hydrothermal treatment, and the number of Al atoms contained in the framework is $36/7 \approx 5$ per unit cell.

(c) Some of the nonframework Al species are still connected with one or two oxygen bridges to Si atoms

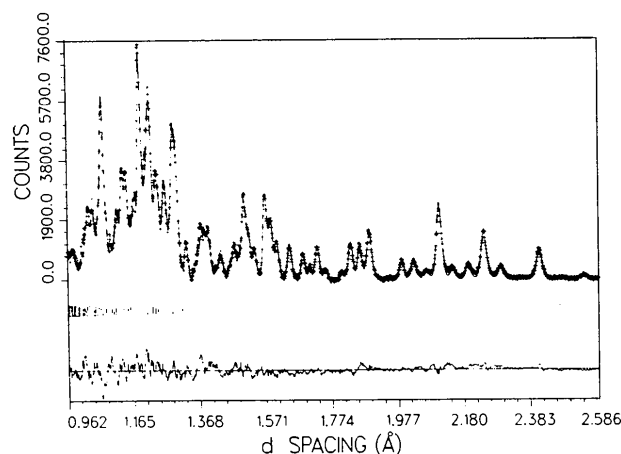


Fig. 4. Observed (crosses) and calculated (line) profile for D-Rho-SS773/RT after background subtraction, with difference plot underneath, showing the deviations between observed and calculated intensities. Tickmarks at the bottom line of the profile indicate peak positions. Only the most crowded part of the profile is shown. Twelve more peaks at $d > 2.6$ Å are omitted from the plot (but were included in the refinement). The profile is drawn after background correction, thus the figure does not show the contribution of the background.

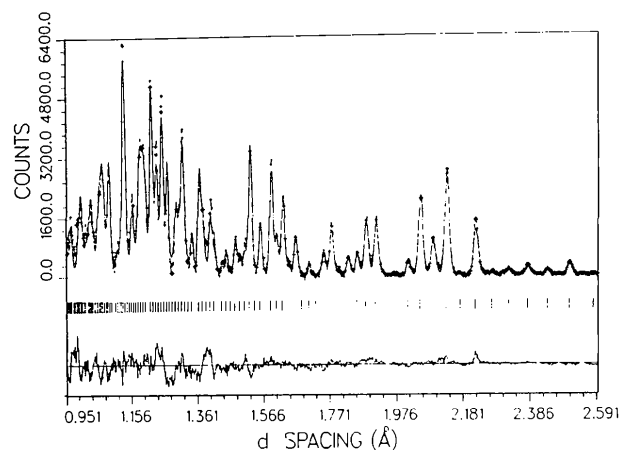


Fig. 5. Observed (crosses) and calculated (line) profile for D-Rho-SS773/623. For explanations see Fig. 4.

in the framework. In this case the Si:Al ratio cannot be derived rigorously from the ^{29}Si peak intensities, as was discussed in our paper on ZK-5 (Fischer *et al.*, 1986b).

We believe that the remarkably high degree of resolution in the ^{29}Si spectrum supports the model of a restored Rho crystal structure with full site occupancy. A rearranged topology would have introduced a highly distorted crystal structure with a wide distribution of $T\text{—O—}T$ angles which would be detected as wide distributions in the ^{29}Si chemical shifts. In addition, the success of the diffraction data refinement shows that we are dealing with a reasonably well crystallized zeolite sample. This supports model (a) where the vacancies are replaced by migrated silicon.

The location of the Al atoms after calcination can be partially inferred from the ^{29}Si and ^{27}Al NMR results (Table 5):

(a) The Al atoms observed by ^{27}Al NMR are still in high-symmetry framework sites.

(b) The Al atoms observed by ^{29}Si NMR as attached to Si atoms (by oxygen bridges) but not observed by ^{27}Al NMR (~5 Al atoms per unit cell) are either in framework sites of distorted symmetry or are outside the framework but still attached to framework Si atoms.

(c) Al atoms not observed by ^{29}Si NMR but determined by the chemical analysis consequently must be either further removed from the framework or completely disconnected from it. They may be attached *via* bridging O atoms to the Al atoms outside the framework (but attached through bridging O atoms to framework Si atoms) or they may be present as a second phase.

The positions of the hydroxyl peaks in the infrared spectra (Fig. 1) and the proton NMR spectra (Fig. 2) are different from the peaks observed for the vacuum-calcined and shallow-bed dry-calcined precursor material. These precursor materials have strong single peaks at 3610 cm^{-1} in the infrared as noted previously (Jacobs & Mortier, 1982) and at 4.0 p.p.m. in the ^1H NMR. This 4.0 p.p.m. ^1H NMR peak has been identified with acidic bridging hydroxyls (Freude, Fröhlich, Pfeifer & Scheler, 1983; Freude, Fröhlich, Hunger, Pfeifer & Scheler, 1983). In H-Rho-SS773 the hydroxyl peak located at 3640 cm^{-1} is associated with a weakly acidic bridging hydroxyl and with the ^1H NMR peak at 2.1 p.p.m. As far as we are aware, this is the first reported instance of a weakly acidic bridging hydroxyl group (Mortier *et al.*, 1984).

Calcination decreased the methanol sorption capacity of D-Rho-SS773 only slightly to 89% of that expected for H-Rho. A reduction of the sorption capacity by 5–10% is believed to result from the amorphitization of the chabazite impurity. Any further reduction is likely to be due to a partial destruction of the Rho phase or to a partial blocking of the zeolitic channels by the aluminium removed from the framework. In the latter case it is not apparent that

simple displacement of aluminium atoms from their framework positions would result in a net decrease in volume.

Framework

Previous refinements of zeolites Rho and ZK-5 (Fischer *et al.*, 1986a,b) have shown an excellent agreement of the observed mean bond lengths $T\text{—O}$ [where T stands for (Si,Al)] with expected values estimated from empirical equations for the Si—O bond length and from the Al content as obtained from MAS NMR. The same is true here (see Table 4). For the mean Si—O bond length we use an empirical equation [equation (8) from Baur (1978)]:

$$(\text{Si—O})_{\text{mean}} = (1.554 + 0.034\text{NSEC}M \\ + 0.0045\text{CN}M)\text{ \AA},$$

where NSEC M is the mean value per tetrahedron of the negative secant of the angle Si—O—Si or Si—O—Al, and CN M is the mean coordination number of all O atoms in the tetrahedron. Taking a value of 2 for CN M and using the (Si,Al)—O—(Si,Al) angles from Table 4 and an Al content of six Al atoms per unit cell we estimate values of about 1.622 Å for $T\text{—O}$ (Table 4). In this it is assumed that the mean Al—O bond length for a tetrahedron in which all O atoms are shared with neighbouring AlO_4 or SiO_4 tetrahedra is 1.746 Å (Baur & Ohta, 1982). The largest difference between observed and estimated mean $T\text{—O}$ bond lengths is only slightly larger than one e.s.d. of an observed mean $T\text{—O}$ distance. Inasmuch as we can view, to a first approximation, the values of $T\text{—O}$ in the three refinements as independent measurements of the same quantity, we really should compare the grand mean value of $T\text{—O}$ of 1.627 Å with the estimated value of 1.622 Å. Considering the probable errors in the observed and estimated $T\text{—O}$ values the agreement is good.

Of special interest is the systematic variation of the mean observed $T\text{—O}$ distances as a function of the status of the refinement. Before the background correction the mean $T\text{—O}$ distances were on average 0.007 Å longer when compared with the same values obtained in the refinement after the background was properly taken care of (Table 2). Upon addition of the nonframework atoms to the model [D, Al(nf), O(nf) and/or Cs] the mean observed $T\text{—O}$ distances were reduced on average by another 0.005 Å. Since this occurred in all three refinements it must be a real effect. This shows the dependence of the framework geometry on the nonframework atoms. As long as a model is still incomplete the refined partial structure might not reflect the real geometry. Unfortunately it is difficult to determine whether or not the model is complete.

We could not find in our structure analyses any evidence for the partial destruction of the framework upon dealumination as reported by Mortier (1983) for a

Table 6. Geometries ($\text{\AA},^\circ$) of bridging OH groups attached to Si and Al atoms

T stands for (Si,Al); Σ is the sum of the $T-O-T$ and $T-O-H$ (or $T-O-D$) angles around the bridging O atoms. The average values are taken only over the more precise values from the three zeolite Rho refinements.

	O-D	T-O	T-O-D	T-O-T	T-D	Σ	Ref.
$H_{52}NaCaAl_{15}Si_{137}O_{384}$ (H-Y)	0.7 (3)	1.60 (5)	106 (20)	147 (3)	1.9 (3)	359	a
La-Y	0.98 (15)	1.64 (5)	112 (4)	130 (3)	2.20 (12)	354	a
D-Rho-SS773/RT	1.2			Not given			b
	1.008 (37)	1.663 (7)	108.1 (17)	140.2 (4)	2.20 (3)	357.5	This work
		1.647 (7)	109.2 (17)		2.20 (3)		
D-Rho-SS773/623	0.955 (21)	1.638 (5)	107.8 (2)	142.2 (3)	2.13 (3)	357.8	This work
D-Rho/W-SS773/RT	0.986 (23)	1.628 (7)	105.2 (4)	142.7 (4)	2.11 (2)	353.1	This work
Average	0.98	1.644	107.6	141.7	2.16	356.1	
Quantum chemical estimate	0.96	1.68 (1)	111.5 (20)	139.1	2.22	359.9	c

References: (a) Jiráček *et al.* (1980). (b) Cheetham *et al.* (1984). H was located in a difference Fourier map, but not refined. Neither coordinates nor chemical composition are given. (c) Mortier *et al.* (1984).

dehydrated sodium/ammonium-exchanged stilbite. The grid search showed some very weak peaks close to O(2) at distances of about 0.4 to 0.6 Å. This might indicate irregularities around O(2), but the distances are too short for interpretation as inverted tetrahedra analogous to those found by Mortier (1983) in stilbite.

Hydroxyl groups

Although the hydroxyl group bridges two T atoms, we cannot state from the diffraction evidence whether the two T are (Al,Al), (Al,Si), or (Si,Si). Hydroxyl groups bridging Si and Al atoms are assumed to occur in zeolites and are probably present in H-Rho-SS773. An OH group bridging two Al is contrary to Loewenstein's rule (Loewenstein, 1954) but that rule was formulated for compounds without OH groups. The sum of the bond strengths (p_O) at the O atom of an OH group would be 2.33 valence units (v.u.) when bonded to two tetrahedrally coordinated Al atoms, 2.58 v.u. when bonded to one Al and one Si neighbor and finally 2.83 v.u. when coordinated to two Si atoms (Baur, 1970). Bond-strength sums higher than that have been observed even in stable structures (Baur, 1970); however, the smaller the deviation from 2 (corresponding to the formal charge of the O atom) the more likely such an arrangement is. An OH group bridging 2 Al has been observed in $AlPO_4-21$ (Parise & Day, 1985), but the Al atoms are five-coordinated in this case, with $p_O = 2.03$ v.u. for the bridging O atom. However, such bond-strength considerations do not prove the existence of an Al-OH-Al bridge.

The results of the structure refinement of D-Rho-SS773/RT and D-Rho/W-SS773/RT confirmed what has been found in D-Rho-SS773/623 (Fischer *et al.*, 1987). The hydroxyl groups exhibit an almost planar geometry together with the T atoms; the sum of the angles around the bridging oxygen is close to 360° (Table 6). The $T-D$ distances range from 2.11 to 2.20 Å. This might seem to be very short, but given an O-D distance of 0.98 Å, the distance $T-D$ cannot be any longer. The $T-D$ distance is determined by the value of the angle $T-O-T$. If hydroxyl groups bridged

the two T atoms making an angle $T-O-T$ larger than the 142° observed here, the $T-D$ distance would be even shorter. The mean values for O-D, $T-O-D$ and $T-D$ observed in Rho are very close to the estimate provided by Mortier *et al.* (1984) on the basis of quantum chemical calculations (Table 6). That estimate was made for a hydroxyl group bridging between Al and Si. Therefore, our observed values are not strictly comparable with that estimate, since what we have observed is the random superposition of Si-O-Si bridges with assumed Si-OH-Al or Al-OH-Al and Si-O-Al bridges. Our crystal structure refinement yielded positions for the centroids of the superposition of these various atoms and therefore the mean $T-O$ distance observed by us is much shorter than the value given by Mortier *et al.* (1984) in their estimate for the Si-O bond. The position of the D atoms of the bridging hydroxyl groups found here corresponds to what we would find if we calculated it on the basis of electrostatic energy minima (Baur, 1965, 1972).

The bond lengths $T-O(1)$ are consistently longer than the $T-O(2)$ bond lengths. This is in keeping with the assumption that the OD groups are concentrated in the O(1) position. However, a quantitative estimate of the bond-length difference between $T-O(1)$ and $T-O(2)$, based on bond-strength considerations (Baur, 1970) shows that $T-O(1)$ should be at most only 0.01 Å longer than $T-O(2)$. This is mainly because only 12 of the 96 $T-O(1)$ bonds per unit cell can be $T-OD$ bonds (given six Al atoms per unit cell). Since $T-O(1)$ exceeds $T-O(2)$ by 0.046 Å in D-Rho-SS773/RT and by 0.026 Å in D-Rho-SS773/623 we must suspect that other nonframework species bond to O(1) as well. Only in the hydrated form (D-Rho/W-SS773/RT) is $T-O(1)$ minus $T-O(2)$ (0.008 Å) of the right magnitude. The AlO species are separated from the framework by the water molecules and the bond lengths within the framework are influenced only by the OD groups.

It is very unlikely that what we see as a bridging OD group is in fact a statistical overlap of terminal OD groups. If this were the case the $T-O(1)$ distance would have to be shorter than the $T-O(2)$ distance, but the

opposite is true. Also we would then expect the temperature factor of atom O(1) to be large. In fact in the two centrosymmetric structures (D-Rho/W-SS773/RT and D-Rho-SS773/623) the temperature factors of O(1) are smaller than those of O(2). Similarly, in the noncentrosymmetric structure (D-Rho-SS773/RT) O(2) has a large value of B [1.5 (1) \AA^2], while O(1) and O(3) have values of 0.9 (1) and 0.8 (1) \AA^2 respectively.

There are many experimental data for terminal hydroxyl groups in silicates (Table 7), but none of them are zeolites. Sixteen single-crystal structure determinations of silicates, three of them by neutron diffraction, have established the geometry of the arrangement well. Interestingly enough, the mean values for all the structure determinations by X-rays are close to the mean values from the neutron diffraction refinements. The grand mean experimental values agree well with the quantum chemical estimate of Mortier *et al.* (1984). Only the estimated value for the Si—O distance is a little too short. However, the prediction that the Si—O—H angle should be larger for terminal hydroxyls than for bridging hydroxyls is borne out. These experimental data for the geometry of terminal hydroxyl groups will become useful for comparative purposes if a zeolite structure displaying terminal hydroxyl groups is determined.

Caesium atoms

Caesium placed on $0.455, 0, 0$ in D-Rho-SS773/623 was refined to an occupancy approximately twice as large as the Cs content determined in the wet chemical analysis. Inasmuch as the temperature factor of this position was held constant in the refinement there is an unknown systematic error in the occupancy factor.

Nonframework aluminium species

The first to report the presence of nonframework aluminium in a dealuminated zeolite on the basis of diffraction data were Maher *et al.* (1971) in an X-ray powder study of dealuminated zeolite Y. Pluth & Smith (1982) reported NFA on the basis of a single-crystal X-ray study of dehydrated Sr-exchanged zeolite A. Parise, Corbin *et al.* (1984) found NFA in a neutron powder diffraction study of a dealuminated zeolite Y. In all these cases the nonframework Al atoms were located in tetrahedral coordination inside the sodalite cages of the zeolite. Shannon *et al.* (1985) determined NFA in a boehmite-like species in the supercages of dehydroxylated zeolite H-Y. This was based on radial distribution studies. Fischer *et al.* (1986*a,b*) found some indication for Al—O—OH clusters in the α cage of zeolite D-Rho and the γ cage of zeolite D-ZK5, both calcined under deep-bed conditions. Further discussion of potential highly condensed aluminium species in zeolites is found in Fischer *et al.* (1986*a,b*). Nonframework aluminium species could be determined in the dehydrated samples

Table 7. Geometries ($\text{\AA},^\circ$) of terminal OH groups attached to Si atoms

When no e.s.d. is stated the H-atom parameters were not varied in the least-squares refinement. In the averaging of the Si—O distances all values were given unit weight. In the averaging of values involving H (or D) all neutron diffraction results (N) were given the same weight as all the X-ray diffraction results (X).

	O—H	Si—O	Si—O—H	Si—H	Method	Ref.
BaSi ₂ O ₈ (OH) ₂ ·2H ₂ O	1.05	1.625 (7)	112	2.24	<i>X</i>	<i>a</i>
	1.05	1.643 (7)	116	2.31	<i>X</i>	<i>a</i>
Na ₇ H ₂ SiO ₈ ·5H ₂ O	0.952 (13)	1.701 (7)	118.6 (9)	2.313 (11)	<i>N</i>	<i>b</i>
	0.933 (11)	1.675 (6)	122.0 (9)	2.309 (11)	<i>N</i>	<i>b</i>
Na ₄ HSiO ₄ ·5H ₂ O	1.07 (5)	1.677 (3)	125 (3)	2.44 (5)	<i>X</i>	<i>c</i>
NaCaHSiO ₄ *	1.00	1.689 (22)	111	2.26	<i>X</i>	<i>d</i>
Na ₂ AlSi ₃ O ₈ OH	0.97 (4)	1.627 (2)	114 (3)	2.21 (4)	<i>X</i>	<i>e</i>
Ca ₃ H ₂ Si ₂ O ₈ ·2H ₂ O	1.19	1.674 (2)	105	2.30	<i>X</i>	<i>f</i>
Na ₇ H ₂ SiO ₈ ·7H ₂ O	0.66 (8)	1.686 (5)	114 (8)	2.05 (8)	<i>X</i>	<i>g</i>
	0.92 (9)	1.642 (5)	114 (7)	2.18 (4)	<i>X</i>	<i>g</i>
Ca ₂ Si ₂ O ₈ (OH) ₂	0.75 (5)	1.648 (1)	111 (3)	2.04 (5)	<i>X</i>	<i>h</i>
	0.99 (3)	1.676 (2)	111 (2)	2.23 (4)	<i>X</i>	<i>h</i>
NaCa ₂ Si ₃ O ₈ OH	1.06 (3)	1.626 (1)	112 (2)	2.25 (4)	<i>X</i>	<i>i</i>
Mn ₂ AsSi ₂ O ₈ OH	0.99	1.650 (6)	121	2.32	<i>X</i>	<i>j</i>
Na ₄ HSiO ₄ ·2H ₂ O	0.97 (3)	1.703 (2)	112 (1)	2.26 (3)	<i>X</i>	<i>k</i>
Na ₄ HSiO ₄ ·2H ₂ O(HT)	0.88	1.685 (3)	122	2.27	<i>X</i>	<i>l</i>
CaMn ₄ (Si ₂ O ₇) ₂ OH·OH ₂ O	0.88	1.624 (2)	116	2.14	<i>X</i>	<i>m</i>
Mn ₂ VSi ₂ O ₈ OH	0.98	1.669 (4)	100	2.08	<i>X</i>	<i>n</i>
Na ₂ D ₂ SiO ₈ ·8D ₂ O	0.977 (3)	1.672 (3)	111.9 (2)	2.230 (3)	<i>N</i>	<i>o</i>
Na ₄ H ₂ SiO ₈ ·4H ₂ O	1.000 (2)	1.668 (1)	116.3 (2)	2.293 (2)	<i>N</i>	<i>p</i>
	0.990 (2)	1.656 (1)	118.3 (1)	2.296 (2)	<i>N</i>	<i>p</i>
Average	0.97	1.663	115.8	2.256		
Quantum chemical estimate	0.95	1.63	115 (2)			<i>q</i>

References: (a) Coda, Dal Negro & Rossi (1967). (b) Williams & Dent Glasser (1971). (c) Smolin, Shepelev & Butikova (1973). (d) Cooksley & Taylor (1974). (e) Rossi, Tazzoli & Ungaretti (1974). (f) Malik & Jeffery (1976). (g) Dent Glasser & Jamieson (1976). (h) Wan, Ghose & Gibbs (1977). (i) Takéuchi & Kudoh (1977). (j) Gramaccioli, Pilati & Liborio (1979). (k) Schmid, Huttner & Felsche (1979). (l) Schmid, Szolnai, Felsche & Huttner (1981). (m) Ohashi & Finger (1981). (n) Gramaccioli, Liborio & Pilati (1981). (o) Schmid, Felsche & McIntyre (1984). (p) Schmid, Felsche & McIntyre (1985). (q) Mortier *et al.* (1984).

* This crystal structure was refined by Cooksley & Taylor (1974) in space group $P2_1$. The correct space group is more likely to be centrosymmetric: $P2_1/m$ (*cf.* Baur & Tillmanns, 1986).

at room temperature and at 623 K. In the hydrated form only deuterium could be detected, which might be a result of the fact that the aluminium species are amorphitized upon hydration.

In D-Rho-SS773/623 the Al(nf) atom has as its next neighbors O(nf) at 1.61 (5) \AA and O(2) at 1.92 (5) \AA . A very distorted tetrahedral coordination is completed by two additional O(2) atoms at 2.51 (4) \AA . There are two more O(2) neighbors at 2.98 (4) \AA . If we count these as coordinating contacts we get an approximately octahedral coordination or alternatively, an AlO^+ group weakly bonded to O(2) of the single six-membered ring. The surroundings of Al(nf) in D-Rho-SS773/RT are similar to those in D-Rho-SS773/623 (Table 4). Here as well, we see essentially only an AlO^+ molecule which is weakly bonded to O atoms of the framework. The mean bond lengths Al(nf)—O are too long for either an octahedral or a tetrahedral environment and the nonframework Al atoms are severely underbonded. On the other hand, the Al(nf) site is not fully occupied and the coordination poly-

hedron of O atoms around it is very distorted. Both these effects tend to increase the apparent mean cation–anion distance (Shannon, 1976).

Within experimental error, framework charge balance in D-Rho-SS773 is achieved by the D^+ ions; therefore, the NFA species must be neutral. The deposition of the *neutral* NFA species Al_2O_3 and $Al_2O_3 \cdot xH_2O$ in the secondary pores of thermally dealuminated zeolite Y was also assumed by Freude, Fröhlich, Hunger *et al.* (1983) and Gross, Lohse, Engelhardt, Richter & Patzelova (1984), respectively. The fact that we assigned the positions to Al and O does not necessarily contradict the assumptions made for the neutrality of the species. The refinement of the nonframework atom positions is extremely affected by the low occupancies, and it is dependent on the symmetry restrictions of the space group; *i.e.* an offset from the mirror plane xxz would allow the theoretical extension of the AlO^+ to a larger molecule, but the refinement did not converge owing to high correlations between the positional parameters. Therefore the standard deviations of the nonframework atom coordinates are not significant and we have to accept a tolerance of at least 0.5 Å for the Al–O positions.

Neutrality can be achieved in various ways:

(a) The AlO might be part of a larger, neutral molecule, which is invisible to us because the missing part is more disordered than the one end which we see bonded to the framework.

(b) The positive charge of the AlO^+ could be compensated by an AlO_2^- ion which could not be determined in the structure analysis.

(c) AlO^+ and AlO_2^- are more or less randomly distributed and only two average positions could be determined.

Provided that aluminium is present as Al^{3+} with a total of six atoms per unit cell as given by NMR (Table 5), the charge balance could be satisfied most simply by either neutral Al_2O_3 molecules or by a combination of three AlO^+ with three AlO_2^- . Such low-condensed AlO species have not been observed in the solid state. However, the formation of a charged AlO^+ molecule has been proposed for a Cu-Y zeolite (Jacobs & Beyer, 1979). Geometrical data on isolated AlO molecules can be found in studies of gaseous Al_2O , AlO and AlO_2 , which are known to be the predominant species present upon evaporation of Al_2O_3 (Bares, Haak & Nibler, 1985; Sonchik, Andrews & Carlson, 1983). Though the vapor species are not directly comparable with the nonframework species in zeolites, they are the only source of geometrical information on isolated aluminium oxygen molecules.

(a) Al_2O^{4+} : proposed Al–O distances are 1.66 Å (Linevsky, White & Mann, 1964), 1.73 Å (Ivanov, Tolmachev, Ezhov, Spiridonov & Rambidi, 1973; Tolmachev & Rambidi, 1973) and 1.87 Å (Woolley, 1959), with an Al–O–Al angle of $\sim 115^\circ$.

(b) AlO^+ : 1.6176 Å (Herzberg, 1950), 1.618 Å (Woolley, Lide & Evans, 1959).

(c) AlO_2^- : the molecule has been observed by Farber & Srivastava (1976), Farber, Srivastava & Uy (1971), Srivastava, Uy & Farber (1972), Persson, Frech & Cedergren (1977) and Rogowski, English & Fontijn (1986), but there are no reported interatomic distances. However, the molecule is expected to be linear as stated in a review of AlO compounds by Carty (1975).

(d) Al_2O_3 : the single molecule is most likely similar to Al_2O , but with terminal oxygen at each end. An isolated Al_2O_3 molecule should be V shaped with a bridging O atom, O(br), at the apex of the V and the two straight sections O(br)–Al–O(ter) making an angle of 148° with each other (Gibbs, 1985, personal communication). Both the bond Al–O(br) and the distance from the Al atom to the terminal O atom, O(ter), should be close to 1.6 Å.

Further evidence for the nature of the aluminium species in zeolite Rho is needed to decide on the configuration actually present in partly dealuminated Rho and whether or not the molecular groups found in this work are part of a larger molecule. In Fig. 6 we show a possible distribution of the nonframework atoms consisting of one Cs atom, six D atoms and six Al–O groups over the unit cell. The positions have been chosen to give sufficiently long interatomic distances (more than 4 Å). Except for this criterion the choice is arbitrary.

It is not clear what effect the NFA has on the bridging OH but its proximity to the OH group in the

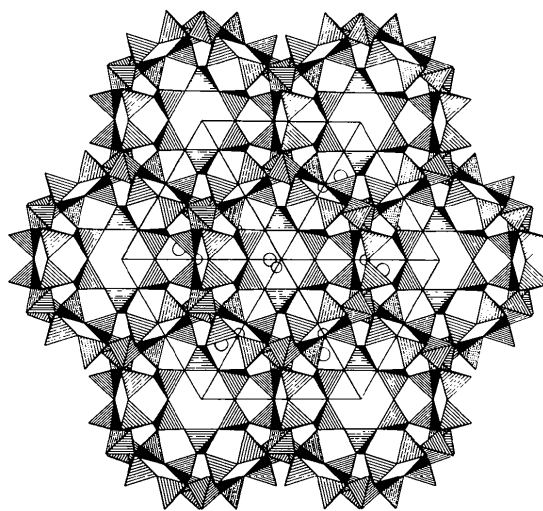


Fig. 6. Projection of the crystal structure of D-Rho-SS773/623 parallel to (111) from -0.5 to 1.5 in all crystallographic directions in polyhedral representation. The outline of the unit cell is indicated. A projection parallel to (100) is given in Fischer *et al.* (1987). The smallest circles represent D atoms bonded to O(1), the medium-sized circles correspond to the Al(nf) atoms, the largest circles to the O atoms, O(nf). Only six of each are shown, see text. Four out of six D atoms are hidden by tetrahedra.

eight-membered ring may be responsible for the unusually low acidity of this group.

Conclusions

Provided that the irregular background is properly treated, neutron powder diffraction of a hydrogenated and dealuminated zeolite Rho gives precise information on bridging hydroxyl groups, and some indication for the presence of nonframework aluminium species formed upon dealumination. The results of this work regarding the nonframework aluminium species are tentative. However, some conclusions emerge clearly. The overall charge of the species must be neutral, as evidenced by NMR and diffraction results which both show all available D⁺ ions attached to the framework. Because of the relatively long T–O(1) distances it has to be assumed that the other nonframework atoms are also bonded to O(1). These additional atoms could not be located in the structure analyses, but might be present as part of a bigger molecule blocking the large channels through the double eight-membered rings.

We thank the North Atlantic Treaty Organization for Research Grant No. 149/84 and the Computer Center of the University of Illinois at Chicago, where part of the work was done, for computer time. In addition RXF and WHB gratefully acknowledge a grant from du Pont de Nemours and Company. One of the authors, JDJ, and the work at the Intense Pulsed Neutron Source were supported by the US Department of Energy, BES–Materials Science, under contract W-31-109-ENG-38. We thank Mrs A. Haake for the drafting of the figures and Mr K. P. Kelber for the photography.

References

- BARES, S. J., HAAK, M. & NIBLER, J. W. (1985). *J. Chem. Phys.* **82**, 670–675.
- BAUR, W. H. (1965). *Acta Cryst.* **19**, 909–916.
- BAUR, W. H. (1970). *Trans. Am. Crystallogr. Assoc.* **6**, 129–155.
- BAUR, W. H. (1972). *Acta Cryst.* **B28**, 1456–1465.
- BAUR, W. H. (1978). *Acta Cryst.* **B34**, 1751–1756.
- BAUR, W. H. & FISCHER, R. X. (1986). *Adv. X-ray Anal.* **29**, 131–142.
- BAUR, W. H., FISCHER, R. X., SHANNON, R. D., STALEY, R. H., VEGA, A. J., ABRAMS, L., CORBIN, D. R. & JORGENSEN, J. D. (1987). *Z. Kristallogr.* **179**, 281–304.
- BAUR, W. H. & OHTA, T. (1982). *Acta Cryst.* **B38**, 390–401.
- BAUR, W. H. & TILLMANN, E. (1986). *Acta Cryst.* **B42**, 95–111.
- BAUR, W. H., WENNINGER, G. & ROY, S. D. (1986). *SADIAN*86. Univ. Frankfurt, Federal Republic of Germany.
- CARTY, A. J. (1975). *MTP International Review of Science, Inorganic Chemistry*, Series 2, Vol. 1, edited by M. F. LAPPERT, pp. 165–218. London: Butterworth.
- CHEETHAM, A. K., EDDY, M. M. & THOMAS, J. M. (1984). *J. Chem. Soc. Chem. Commun.* pp. 1337–1338.
- CODA, A., DAL NEGRO, A. & ROSSI, G. (1967). *Atti. Accad. Naz. Lincei Cl. Sci. Fis. Mat. Nat. Rend.* **42**, 859–873.
- COOKSLEY, B. G. & TAYLOR, H. F. W. (1974). *Acta Cryst.* **B30**, 864–867.
- DENT GLASSER, L. S. & JAMIESON, P. B. (1976). *Acta Cryst.* **B32**, 705–710.
- FARBER, M. & SRIVASTAVA, R. D. (1976). *Combust. Flame*, **27**, 99–105.
- FARBER, M., SRIVASTAVA, R. D. & UY, O. M. (1971). *J. Chem. Phys.* **55**, 4142–4143.
- FISCHER, R. X. (1985). *J. Appl. Cryst.* **18**, 258–262.
- FISCHER, R. X., BAUR, W. H., SHANNON, R. D. & STALEY, R. H. (1987). *J. Phys. Chem.* **91**, 2227–2230.
- FISCHER, R. X., BAUR, W. H., SHANNON, R. D., STALEY, R. H., VEGA, A. J., ABRAMS, L. & PRINCE, E. (1986a). *J. Phys. Chem.* **90**, 4414–4423.
- FISCHER, R. X., BAUR, W. H., SHANNON, R. D., STALEY, R. H., VEGA, A. J., ABRAMS, L. & PRINCE, E. (1986b). *Zeolites*, **6**, 378–387.
- FLOCKHART, B. D., MEGARRY, M. C. & PINK, R. C. (1973). In *Molecular Sieves*, Advances in Chemistry Series No. 121, edited by W. M. MEIER & J. B. UYTTERHOEVEN, pp. 509–517. Washington, DC: American Chemical Society.
- FREUDE, D., FRÖHLICH, T., HUNGER, M., PFEIFER, H. & SCHELER, G. (1983). *Chem. Phys. Lett.* **98**, 263–266.
- FREUDE, D., FRÖHLICH, T., PFEIFER, H. & SCHELER, G. (1983). *Zeolites*, **3**, 171–177.
- GEERLINGS, P., TARIEL, N., BOTREL, A., LISSILLOUR, R. & MORTIER, W. J. (1984). *J. Phys. Chem.* **88**, 5752–5759.
- GHOSE, S. & TSANG, T. (1973). *Am. Mineral.* **58**, 748–755.
- GRAMACCIOLI, C. M., LIBORIO, G. & PILATI, T. (1981). *Acta Cryst.* **B37**, 1972–1978.
- GRAMACCIOLI, C. M., PILATI, T. & LIBORIO, G. (1979). *Acta Cryst.* **B35**, 2287–2291.
- GROSS, T., LOHSE, U., ENGELHARDT, G., RICHTER, K. H. & PATZELOVA, V. (1984). *Zeolites*, **4**, 25–29.
- HERZBERG, G. (1950). *Molecular Spectra and Molecular Structure. I. Spectra of Diatomic Molecules*, p. 504. Princeton, NJ: Van Nostrand.
- International Tables for Crystallography* (1983). Vol. A, pp. 653, 703. Dordrecht: D. Reidel (Present distributor Kluwer Academic Publishers, Dordrecht.)
- IVANOV, A. A., TOLMACHEV, S. M., EZHOV, YU. S., SPIRIDONOV, V. P. & RAMBIDI, N. G. (1973). *J. Struct. Chem. (USSR)*, **14**, 854–856.
- JACOBS, P. A. & BEYER, H. K. (1979). *J. Phys. Chem.* **83**, 1174–1177.
- JACOBS, P. A. & MORTIER, W. J. (1982). *Zeolites*, **2**, 226–230.
- JIRÁK, Z., VRATISLAV, S. & BOSÁČEK, V. (1980). *J. Phys. Chem. Solids*, **41**, 1089–1095.
- JORGENSEN, J. D. & FABER, J. (1983). *Proc. 6th Meet. Int. Colloq. Adv. Neutron Sources*, ANL-82-80, pp. 105–114. Argonne: Argonne National Laboratory.
- KERR, G. T. (1973). In *Molecular Sieves*, Advances in Chemistry Series No. 121, edited by W. M. MEIER & J. B. UYTTERHOEVEN, pp. 219–229. Washington, DC: American Chemical Society.
- KLINOWSKI, J. (1984). *Prog. Nucl. Magn. Reson. Spectros.* **16**, 237–309.
- KOESTER, L. (1977). *Springer Tracts Mod. Phys.* **80**, 1–55.
- LINEVSKY, M. J., WHITE, D. & MANN, D. E. (1964). *J. Chem. Phys.* **41**, 542–545.
- LOEWENSTEIN, W. (1954). *Am. Mineral.* **39**, 92–96.
- MCCUSKER, L. B. (1984). *Zeolites*, **4**, 51–55.
- MCCUSKER, L. B. & BAERLOCHER, C. (1984). *Proc. 6th Int. Zeolite Conf.*, edited by D. OLSON & A. BISIO, pp. 812–822. Guildford: Butterworth.
- MAHER, P. K., HUNTER, F. D. & SCHERZER, J. (1971). In *Molecular Sieve Zeolites I*, Advances in Chemistry Series No. 101, edited by E. M. FLANIGAN & L. B. SAND, pp. 266–278. Washington, DC: American Chemical Society.
- MALIK, K. M. A. & JEFFERY, J. W. (1976). *Acta Cryst.* **B32**, 475–480.
- MORTIER, W. J. (1983). *Am. Mineral.* **68**, 414–419.

- MORTIER, W. J., SAUER, J., LERCHER, J. A. & NOLLER, H. (1984). *J. Phys. Chem.* **88**, 905–912.
- OHASHI, Y. & FINGER, L. W. (1981). *Am. Mineral.* **66**, 154–168.
- PARISE, J. B., CORBIN, D. R., ABRAMS, L. & COX, D. E. (1984). *Acta Cryst.* **C40**, 1493–1497.
- PARISE, J. B. & DAY, C. S. (1985). *Acta Cryst.* **C41**, 515–520.
- PARISE, J. B., GIER, T. E., CORBIN, D. R. & COX, D. E. (1984). *J. Phys. Chem.* **88**, 1635–1640.
- PERSSON, J., FRECH, W. & CEDERGRÉN, A. (1977). *Anal. Chim. Acta*, **92**, 85–93.
- PLUTH, J. J. & SMITH, J. V. (1982). *J. Am. Chem. Soc.* **104**, 6977–6982.
- RIETVELD, H. M. (1969). *J. Appl. Cryst.* **2**, 65–71.
- ROBSON, H. E., SHOEMAKER, D. P., OGILVIE, R. A. & MANOR, P. C. (1973). In *Molecular Sieves*, Advances in Chemistry Series No. 121, edited by W. M. MEIER & J. B. UYTTERHOEVEN, pp. 106–115. Washington, DC: American Chemical Society.
- ROGOWSKI, D. F., ENGLISH, A. J. & FONTUN, A. J. (1986). *J. Phys. Chem.* **90**, 1688–1691.
- ROSSI, G., TAZZOLI, V. & UNGARETTI, L. (1974). *Am. Mineral.* **59**, 335–340.
- ROTELLA, F. J. (1982). *Users Manual for Rietveld Analysis of Time-of-Flight Neutron Powder Data at IPNS*. Argonne: Argonne National Laboratory.
- SCHMID, R. L., FELSCHE, J. & MCINTYRE, G. J. (1984). *Acta Cryst.* **C40**, 733–736.
- SCHMID, R. L., FELSCHE, J. & MCINTYRE, G. J. (1985). *Acta Cryst.* **C41**, 638–641.
- SCHMID, R., HUTTNER, G. & FELSCHE, J. (1979). *Acta Cryst.* **B35**, 3024–3027.
- SCHMID, R. L., SZOLNAI, L., FELSCHE, J. & HUTTNER, G. (1981). *Acta Cryst.* **B37**, 789–792.
- SHANNON, R. D. (1976). *Acta Cryst.* **A32**, 751–767.
- SHANNON, R. D., GARDNER, K. H., STALEY, R. H., BERGERET, G., GALLETOT, P. & AUROUX, A. (1985). *J. Phys. Chem.* **89**, 4778–4788.
- SMOLIN, YU. I., SHEPELEV, YU. F. & BUTIKOVA, I. K. (1973). *Sov. Phys. Crystallogr.* **18**, 173–176.
- SONCHIK, S. M., ANDREWS, L., & CARLSON, K. D. (1983). *J. Phys. Chem.* **87**, 2004–2011.
- SRIVASTAVA, R. D., UY, O. M. & FARBER, M. (1972). *J. Chem. Soc. Faraday Trans. 2*, **68**, 1388–1392.
- TAKÉUCHI, Y. & KUDOH, Y. (1977). *Z. Kristallogr.* **146**, 281–292.
- TOLMACHEV, S. M. & RAMBIDI, N. G. (1973). *High Temp. Sci.* **5**, 385–394.
- VEGA, A. J. & LUZ, Z. (1987). *J. Phys. Chem.* **91**, 365–373.
- VON DREELE, R. B., JORGENSEN, J. D. & WINDSOR, C. G. (1982). *J. Appl. Cryst.* **15**, 581–589.
- WAN, C., GHOSE, S. & GIBBS, G. V. (1977). *Am. Mineral.* **62**, 503–512.
- WILLIAMS, P. P. & DENT GLASSER, L. S. (1971). *Acta Cryst.* **B27**, 2269–2275.
- WOOLLEY, H. W. (1959). *Natl Bur. Stand. (US) Rep.* No. 6484, 40–44.
- WOOLLEY, H. W., LIDE, D. R. & EVANS, W. H. (1959). *Natl Bur. Stand. (US) Rep.* No. 6484, 45–48.

Acta Cryst. (1988). **B44**, 334–340

New Analysis of the Neutron Diffraction Data for Anhydrous Orthophosphoric Acid and the Structure of H₃PO₄ Molecules in Crystals

BY ROBERT H. BLESSING

Medical Foundation of Buffalo, 73 High Street, Buffalo, New York 14203, USA

(Received 14 September 1987; accepted 2 February 1988)

Abstract

Two neutron data sets, which had been analyzed separately to determine the H-atom positions in H₃PO₄ crystals [Cole (1966), PhD Thesis, Univ. of Washington, Pullman, USA], have been re-analyzed in a joint refinement, fitting separate scale and extinction parameters for each data set, in order to obtain more precise positional and vibrational parameters. The new refinement gave $R(F) = 0.036$ for the combined 743 data. For the new results, and for six other H₃PO₄ molecules from four other, different crystal structures, thermal vibration analyses have been performed, and the molecular structures, thermal vibrations and hydrogen-bonding effects are compared. The rigid-body model is found to be better than the riding model for the PO₄ groups. The P–OH bond lengths are markedly affected by hydrogen bonding, but seem to be independent of O=P–O–H conformation. These effects are interpreted in terms of the P–O partial double-bond

character. Crystal data (Cole, 1966): anhydrous orthophosphoric acid, H₃PO₄, $M_r = 98.00$, room temperature, $P2_1/c$, $a = 5.779$ (9), $b = 4.826$ (4), $c = 11.606$ (40) Å, $\beta = 95.26$ (18)°, $V = 322.3$ (20) Å³, $Z = 4$, $D_x = 2.019$ mg mm⁻³, $\mu = 0.1687$ mm⁻¹ for neutrons with $\lambda = 1.450$ Å.

Introduction

The general features of the H₃PO₄ crystal structure were worked out from two-dimensional X-ray data by Smith, Brown & Lehr (1955) and, independently, by Furberg (1955). The H-atom positions were determined from three-dimensional neutron data by Cole (1966) [see also Cole & Peterson (1964)].

Cole (1966) carried out separate structure refinements against two neutron data sets measured at different wavelengths. One refinement, against 482 data with $(\sin\theta_{\max})/\lambda = 0.56$ Å⁻¹ at $\lambda = 1.450$ Å, gave R